Adding Scattering to the UCSB Broadband Modeling Method

Report for SCEC Award #15069
Submitted March16, 2016

Investigators: Ralph Archuleta (UCSB), Jorge Crempien (UCSB)

I. Project Overview

A. Abstract

In the box below, describe the project objectives, methodology, and results obtained and their significance. If this work is a continuation of a multi-year SCEC-funded project, please include major research findings for all previous years in the abstract. (Maximum 250 words.)

The primary objective was to improve the UCSB method for computing broadband ground motion synthetics by adding scattering to the wave propagation. We have done this by generating scatterograms that are added to the Green's function for the medium. The scatterogram is obtained by using Zeng's (1991) envelope for multiple scatterers to modify a white noise signal. The advantage of this method is that the parameters for the envelope can be determined from regional, small magnitude earthquakes. Thus the scattering is constrained by empirical data that is germane to the region where the larger magnitude earthquake is simulated. This approach allows the UCSB broadband method to capture the duration of shaking that is due to both the duration of the source process as well as the duration due to scattering in the medium. Using the 1994 Northridge earthquake we have shown that this scattering does not affect the bias when comparing response spectra of spectral acceleration. However, it greatly reduces the bias of Arias intensity—a measure that includes both amplitude and duration of shaking. In earlier work we have shown that the UCSB method has successfully passed the SCEC validation process for western crustal earthquakes.

B. SCEC Annual Science Highlights

Ground Motion Prediction (GMP)
Ground Motion Simulation Validation (GMSV)
Central California Seismic Project (CCSP)

C. Exemplary Figure

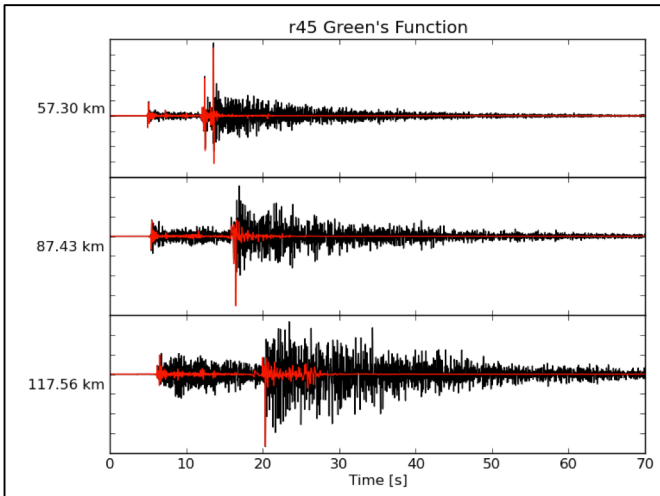

Figure 1: Comparison between deterministic (red) and scattering (black) Green's functions at different epicentral distances for a point source (reverse faulting with 45° dip) at a depth of 10 km.

D. SCEC Science Priorities

6c, 6d, 6e

E. Intellectual Merit

One of the overarching SCEC goals is the development of a seismic hazard model for Southern California. One cornerstone of a seismic hazard model is the prediction of ground motion (or a metric based on ground motion). Over many years SCEC has supported the development of numerical methods by which ground motion from simulated earthquakes can be computed. One such method has been developed at UCSB. The UCSB method differs from others in that the slip rate function (spatially varying on the fault) determines the entire frequency spectrum of the ground motion, i.e., the low-frequency and the high-frequency parts of the ground motion are all determined by the slip rate on the fault. There is no disconnect between the source of low- and high-frequency source. To improve on this method we have modified how high-frequency ground motion is propagated. In the latest modification we have added scattering to the wave propagation. In this approach we can use scattering parameters that are empirically determined from small earthquakes. We have found that this greatly improves estimates of duration of shaking; duration is a critical time-domain ground motion metric.

F. Broader Impacts

Earthquake engineering design depends on having reliable and verifiable estimates of how strong shaking will be for a wide suite of earthquake magnitudes and distances. While the database of strong motion records has been increasing with new instrumentation, there is a serious lack of ground motion records at distances less than 20 km for earthquakes with magnitudes greater than 6.0. Rather than wait for more earthquakes to occur, it is possible to estimate ground motion by simulating earthquakes of different magnitudes. Thus one can supplement the empirical database and incorporate region specific geology by computing ground motion using numerical simulations of earthquakes.

G. Project Publications

Crempien, J. G. F., and R. J. Archuleta (2014). Inclusion of nonstationary coda in time and frequency for computing synthetic ground motions from earthquake scenarios. 2014 SSA annual meeting.

II. Technical Report

A. Overview

Green's functions computed for 1D velocity structures are not able to reproduce the coda amplitudes observed in real seismograms. Because synthetic ground motion lack of this coda, we show that at close distances to the fault, ground motion duration based on the Arias intensity measure is considerably lower than observed.

To include coda in the synthetic seismograms we make use of non-stationary observations of scattering impulse response functions (SIRF's) at different frequencies to simulate synthetic scatterograms based on the theory of sigma oscillatory processes (Priestley, 1965). This model assumes that a stochastic signal can be represented as a non-stationary process both in time and frequency (Equation 1):

$$s(t) = \int_0^\infty A(t,\omega) e^{i\omega t}\, dZ(\omega) \ . \tag{1}$$

We add the synthetic scatterogram realizations to our deterministic Green's functions. The envelope functions are the SIRF's. They are chosen based on the distance between an element on the fault and the station, and the frequency band. With these modified Green's functions, we use the representation theorem to compute ground motion with the UCSB method (Schmedes *et al*., 2013; Crempien and Archuleta, 2015).

We validated our synthetic ground motion model by computing the bias between spectral acceleration of recorded and synthetic ground motions for the 1994 Northridge earthquake. Our results show negligible bias in both period and distance. At the same time, we validate our method by showing that the bias of ground motion duration, based on evolutionary Arias intensity, is negligible.

1. Problem Setup

We use a modulating function in both frequency and time to simulate synthetic scatterograms based on Priestley's (1965) work. We implement a discretization scheme proposed by Preumont (1985), such that the for each frequency band, we simulate a stationary normal distribution white noise that is band-passed for each frequency band as shown in the Equation (2).

$$s(t) = \sum_{i=1}^{M} \phi_i(t) x(t) \tag{2}$$

where $\phi_i(t)$ are deterministic modulating functions for each frequency band, $x_i(t)$ are stochastic realizations of normally distributed Gaussian white noise, band-passed in the corresponding i^{th} frequency band, and *M* is the number of frequency bands. The envelope function defined by Zeng (1991) to model only the S-wave scattering process is shown the Equation (3).

$$\begin{aligned} E(r,t) = {} & E_0 e^{-\eta v t}\left[\frac{\delta(t-r/v)}{4\pi v r^2} + \frac{\eta_s H(t-r/v)}{4\pi v t}\ln\left(\frac{1+r/(vt)}{1-r/(vt)}\right)\right] \\ & + cH\left(t-\frac{r}{v}\right)\left(\frac{3\eta_s}{4\pi v t}\right)^{3/2} e^{\frac{3\eta_s r^2}{4vt} - \eta_i v t} \end{aligned} \tag{3}$$

where E_0 is the total incident wave energy, v is the shear wave velocity, r is the traveled distance, η_i and η_s are the absorption and scattering coefficients and $\eta = \eta_i + \eta_s$. To simulate scatterograms, we first define *E(r,t)* for each station-subfault pair and frequency band. After the Envelope functions are defined, we use Equation (2) to simulate synthetic scatterograms such that the modulating function equals the square root in time of the envelope functions as $\phi_i(t) = (E_i(r,t))^{1/2}$. The final process consists in normalizing each scatterogram to the FAS of the direct arrival in Zeng's (1991) envelope in Equation (3). Once the scatterograms are constructed for each station-subfault pair, we convolve them with the corresponding Green functions and add the resultant stochastic realization to the Green's functions, as shown in Equation (4).

$$g_s(r,t) = g(r,t) + g(r,t) * s_n(r,t) \quad (4)$$

where $g_s(r,t)$ is the Green's function with scattering, $g(r,t)$ is the deterministic Green's function computed with a discrete wavenumber technique using a 1D velocity structure and $s_n(r,t)$ is the normalized scatterogram of the direct arrival (Equation 5), which corresponds to the first term of Zeng's (1991) equation.

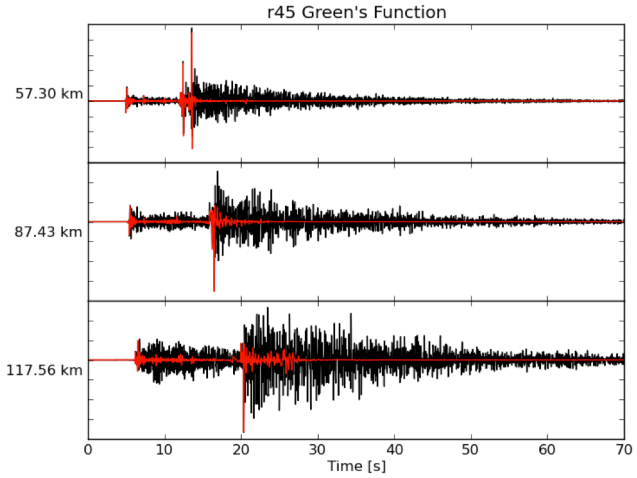

Figure 1: Comparison between deterministic (red) and scattering (black) Green's functions at different epicentral distances for a point source (reverse faulting with 45˚ dip) at a depth of 10 km.

$$\tilde{s}_n(r,\omega) = \tilde{s}(r,\omega) / \tilde{h}(\omega)$$

$$\tilde{h}(\omega) = FT\left(e^{-\nu t L_e^{-1}} \times \frac{\delta(t - t_s)}{4\pi\nu r^2} \right) \quad (5)$$

This technique preserves the main phases that are attributed to specific rays that travel within the 1D crustal model. In Figure 1 we show three Green's functions at epicentral distances of 57.3, 87.43 and 117.56 km computed for a point source (reverse mechanism with a 45˚ dip) at a depth of 10 km. The red curve is the Green's function and the black curve corresponds to the stochastic Green's functions (SGF's). We use the intrinsic and scattering Q results of Jin *et al.* (1994) to simulate synthetic scatterograms.

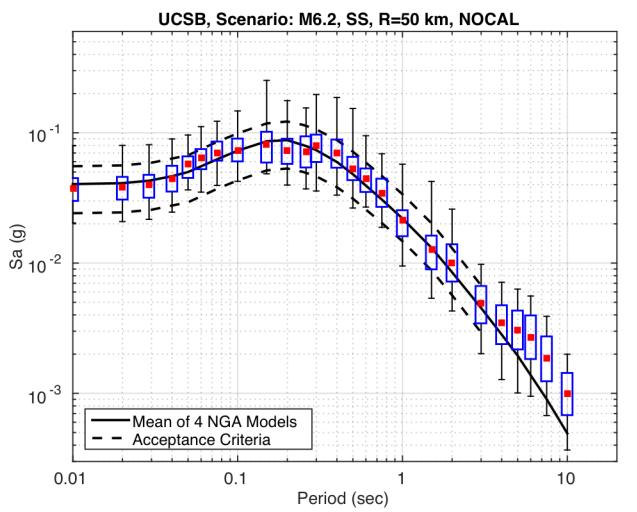

Figure 2: We show the statistics of 16 realizations of a **M** 6.2 strike-slip, where the median RotD50 spectrum is depicted as a red dot at each period for all stations. The blue boxes represent 90% confidence intervals of mean and the black whiskers are the extrema of the 50 simulations for all stations and realizations. The black solid line is the average of the four 2008 NGA-West1 GMPE models, as described in Goulet et al. (2015). In all plots, results are for a set

2. Main Results

In Figure 2 we show the mean (and standard deviation) acceleration response spectra from 50 realizations of a **M** 6.2 strike-slip earthquake compared with the mean GMPE prediction. The red dots correspond to the mean of RotD50 spectra of all realizations at each period. The blue boxes are the 90% confidence intervals of the realizations and the whiskers show the maxima and minima of the realizations. The black solid line corresponds to the mean of the 2008 NGA GMPE models and the dashed line corresponds to the limits of acceptability of the synthetic ground motion for the SCEC validation exercise (Goulet *et al.*, 2015). These results show almost no variation compared with the original results of the UCSB model shown in Crempien and Archuleta (2015). These results capture the ground motion intensities predicted by the NGA GMPE's. We can still see higher amplitudes at the longer periods—a feature already identified by Crempien and Archuleta (2015) as over prediction due to the use of 1D crustal structure, which naturally creates and amplifies surface waves for frequencies below 1.0-0.5 Hz.

When we compare our synthetic simulations with the 1994 **M**6.7 Northridge earthquake observed ground motions, we still observe no

significant differences between the RotD50 spectral amplitudes of our model with and without scattering. In Figure 3 we show results with and without scattering of the combined bias for all stochastic realizations and stations for each period. The black line corresponds to the mean bias; the magenta region is the 90% confidence interval of the mean bias; and the lavender region shows the standard deviation around the mean.

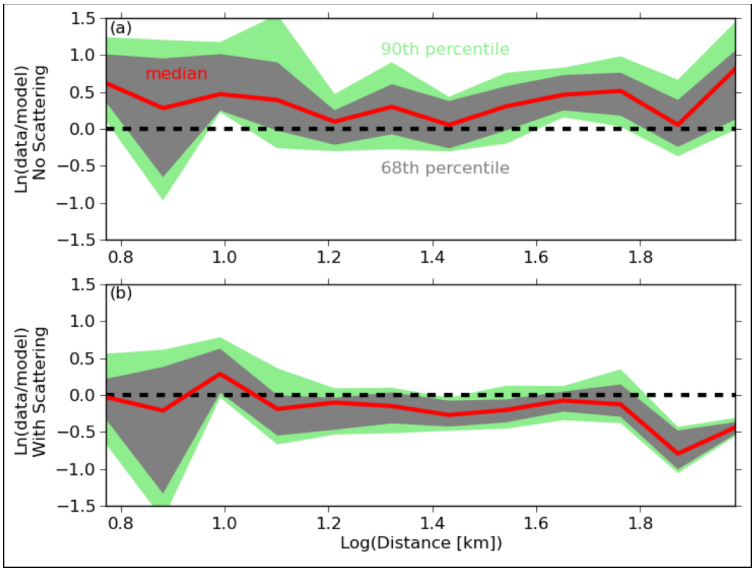

Figure 4: (a) and (b) show the log-bias between synthetic and observed ground motion duration without and with scattering, respectively, versus distance. The duration is based on the time between 5 and 75% of the total Arias intensity. The red line corresponds to the median of duration, the grey and light grey areas correspond to the 68th and 90th percentile respectivley. The statistics are drawn at different bins of closest distance from station to the fault and 16 realizations.

These results are promising because our primary goal is to capture with our model the observed ground motion intensity measures (GMI's) related to response spectrum. However, there are also important GMI's related to strong ground motion durations that should be captured as well by the model, specifically, the duration of ground motion based on Arias intensity. We have chosen to check the duration between 5 and 75% of the total Arias intensity (Figure 4). The original model underestimates ground motion duration by almost 0.5 in natural logarithmic scale. The model that includes scattering produces a much better estimate of Arias intensity (Figure 4b), with the exception of the furthest stations. The over-prediction at larger distances is mostly seen at stations that are in the Mojave Desert on the eastern side of the San Gabriel Mountains. The decrease of SIRF amplitude across mountain ranges has been previously observed for Lg and scattered Lg waves (across the Alpine Range) by Campillo *et al*. (1993) and Eva *et al*. (1991).

B. References

Campillo, M., B. Feignier, M. Bouchon, and N. Béthoux (1993). Attenuation of crustal waves across the Alpine Range, *J. Geophys. Res.*, **98**, B2, 1987-1996, doi:10.1029/92JB02357.

Crempien, J. and R. J. Archuleta (2015). UCSB synthetic broadband ground motion method for kinematic simulations of earthquakes, *Seismol. Res. Lett.*, **86**, 1, 61-67, doi:10.1785/0220140103.

Eva, C., M. Cattaneo, P. Augliera, and M. Pasta (1991). Regional coda Q variations in the western Alps (northern Italy), *Phys. Earth Planet. Inter.*, **67**, 76-86.

Goulet, C. A., and N. A. Abrahamson (2015). The SCEC broadband platform validation exercise for pseudo-spectral acceleration: methodology for code validation in the context of seismic hazard analyses, *Seismol. Res. Lett.*, **86**, 1, 17-26, doi:10.1785/0220140104.

Jin, A., K. Mayeda, D. Adams, and K. Aki (1994). Separation of intrinsic and scattering attenuation in southern California using TERRAscope data, *J. Geophys. Res.*, **99**, 17835-17848.

Preumont, A. (1985). The generation of non-separable artificial earthquake accelerograms for the design of nuclear power plants, *Nuclear Engineering and Design*, **88**, 59-67.

Priestley, M. B. (1965). Evolutionary spectra and non-stationary processes, *J. Royal Statistical Society*, **27**, 204-237.

Schmedes, J., R. J. Archuleta, and D. Lavallée (2013). A kinematic rupture model generator incorporating spatial interdependency of earthquake source parameters, *Geophys. J. Int.* **192** (3), 1116-1131. doi: 10.1093/gji/ggs02.

Zeng, Y. (1991). Compact solutions for multiple scattered wave energy in time domain, *Bull. Seismol. Soc. Am.*, **81**, 1022-1029.